processes

MDPI

Article

Ageing Studies of Pt- and Pd-Based Catalysts for the Combustion of Lean Methane Mixtures

Georgeta M. Istratescu and Robert E. Hayes *

Department of Chemical and Materials Engineering, University of Alberta, Edmonton, AB T6G 2G6, Canada; istrates@ualberta.ca
* Correspondence: hayes@ualberta.ca

Abstract: This paper presents results obtained for the thermal and hydrothermal ageing of seven commercial precious metals-based catalysts for the combustion of methane. Experiments are performed in a large excess of oxygen representing lean conditions. Temperatures used are those typically found in lean burn compression ignition engines. The precious metals used were platinum, palladium and rhodium, present either singly or in combination. The most active catalyst contains a platinum and palladium mixture, with palladium being dominant. This catalyst was also the least affected by both thermal and hydrothermal ageing. The second most active catalyst contained only palladium, but this catalyst also demonstrated more susceptibility to ageing. The least active catalyst contained only platinum, although this catalyst was also the least affected by hydrothermal ageing. The addition of rhodium to either palladium or platinum–palladium catalysts caused a more rapid loss in activity at higher temperatures, although the loss in activity at lower temperatures was similar in magnitude to those catalysts without rhodium. In some cases, cycling the reactor temperature between high and low restored some activity to the catalyst. In all cases, the catalyst activity was observed to be lower in the presence of water, after both thermal and hydrothermal ageing.

Keywords: lean burn; catalytic combustion; fugitive emissions; natural gas engine

Citation: Istratescu, G.M.; Hayes, R.E. Ageing Studies of Pt- and Pd-Based Catalysts for the Combustion of Lean Methane Mixtures. *Processes* **2023**, *11*, 1373. https://doi.org/10.3390/pr11051373

Academic Editor: Elio Santacesaria

Received: 20 March 2023
Revised: 24 April 2023
Accepted: 27 April 2023
Published: 1 May 2023

1. Introduction

Catalytic combustion has been known since the original observations of Sir Humphry Davy, and it can be used as an alternative to conventional (homogeneous) combustions in cases where low temperature combustion is desired, or the fuel content lies outside of the flammability limits [1–3]. Catalytic combustion can be used in a wide variety of applications. For example, catalytic combustion can be used as a means of lowering NO_X emissions [4], and during the 1990s there was a considerable interest in the use of catalytic combustion for gas turbine applications [5–7]. As the century turned, interest was growing in the use of catalytic combustion as a means of controlling fugitive emissions of VOC, especially methane, in a large part because of the large global warming potential of methane. Fugitive methane emissions are present in fossil fuel development, and catalytic combustion has been suggested as a means to destroy them [8]. Emissions from this sector may be dry or contain small amounts of water.

Another major focus for the catalytic combustion of methane is the desire to use methane as a replacement for either diesel or gasoline as a fuel in internal combustion engines. There is a similar problem of methane slip from engines powered by biogas, which also require an emission control solution. This interest is found not only in Europe and North America, but also in large markets such as India and China. Natural gas is an alternative fuel for low emission transportation because it burns the most cleanly of all of the fossil fuels, with near zero particulate matter, and lower greenhouse gas emissions [3]. Natural gas can be used effectively in compression ignition (CI) engines, which typically operate in the lean combustion regime, and also in spark ignition (SI) engines which usually run with stoichiometric air to fuel ratios.

Because of incomplete combustion, the exhaust from natural gas-fuelled vehicles contains an unacceptable level of methane which must be oxidized by using a catalytic convertor. Methane is a regulated emission; therefore, the development of a high efficiency catalytic convertor for a natural gas engine is required. This task is a challenge, owing to the low reactivity of methane and the presence of large amounts of water vapour in the exhaust. SI and CI engines operate in quite different modes, and the exhaust gas after treatment systems are quite different in each case. In this work, the focus is on CI engines, which typically operate with lower combustion temperatures (300 to 500 °C) than SI engines, and the trend is to push for lower temperatures to reduce emissions, especially of NO_X. Exhaust gas recirculation may also be used.

Some exhaust system designs have been proposed in which recuperative heat transfer or energy addition is used as a means of increasing the temperature of the catalytic converter to enhance the reaction rate [9–11], although these methods add complexity to the exhaust system. To avoid this complexity, a catalyst that is active at low temperatures and is resistant to deactivation both in the presence and the absence of water is desirable.

Many catalysts have been reported in the literature for methane oxidation, which can be broadly classed into those based on non-noble metals and those based on the use of precious group metals (PGM) [12]. For reasons of both cost and high temperature durability, interest has been continuous in earth abundant elements, see for example [13–21]. Many applications, and especially automotive catalytic converters, must have a reactor with a small physical size, and therefore a very active catalyst is required. Thus, the use of various PGM group metals has been actively explored, as summarized in several reviews over the past decades [22–26]. Platinum, which is widely used in automotive catalytic converters for gasoline and diesel engines, has also been studied for the catalytic combustion of methane [27–33]. Platinum has also been combined with earth common metals [34]. A notable industrial application of Pt catalysts in methane combustion are the fibre-supported catalysts used in counter diffusive catalytic heaters [35,36]. The most commonly used uni-metallic methane combustion catalyst is palladium, and papers using it account for the majority of the papers extant, as can be observed from the reviews cited above. A wide variety of factors that affect the activity of Pd (and other PGM) catalysts have been studied, and some references are given in the following paragraphs.

Whilst the active catalytic ingredient is clearly important, the role of the catalyst support has long been recognized [37–40] and recently the subject of a comprehensive review [41]. A wide variety of materials has been used, with alumina being common [42–49]; however, zirconia [50–54], silica [55–57], aluminosilicates [58], cobalt oxide [59,60], ceria [61,62], nickel compounds [63] and tin are also used [64,65]. The support material is important, but so also is the preparation method [66–68]. In addition to the main ingredient and the support, other materials have been added as promoters [69–71].

Introducing a second metal component into a heterogeneous has been widely accepted as one of the ways to increase activity, selectivity and/or stability. Other PGM have been incorporated into methane combustion catalysts. For example, rhodium, which is used in the three-way catalyst, has been combined with Pd [72–74] and Pt [75,76]. Gold has also been reported for Pd [77,78] and Pt [79], although to the best knowledge of the authors has not been commercially applied. Arguably, the most commonly reported bimetallic PGM catalyst is the mixture of Pd and Pt [73,80–86]. The use of the bimetallic introduces as a variable the ratio of Pd and Pt used, and this variable has been studied [80,87–90]. Generally speaking, the addition of Pt to Pd gives a more active catalyst that is less prone to deactivation [91–93]. As with Pt, non-PGM metals have also been added to Pd catalysts [94].

The exhaust gas from a natural gas engine contains of the order of 10 to 15% by volume water. The activity of the catalyst in the presence of water is thus of the utmost importance, and is related to the deactivation of the catalyst [37,95–103]. It has been suggested that the water inhibition is only significant up to approximately 450 °C [24,103–106]. It has been suggested that this temperature limit results from the formation of inactive $Pd(OH)_2$ [52,107]. Water may also affect the oxidation state of Pd during the reaction, reducing the speed of reoxidation of

Pd to PdO [92,108]. The sintering of the metal particles as a result of temperature and/or the atmosphere also affects the catalyst activity [109]. It has been reported that the oxidation of methane over Pd is structure-sensitive [49]. As noted, water affects catalyst deactivation, and also inhibits the oxidation reaction. The work reported here follows from two publications that considered the combustion of methane over Pt:Pd catalysts. Abbasi [110] reported some kinetic models over two Pt-based catalysts, one of which was a Pt:Pd blend containing 20% by weight palladium. Abbasi [111] investigated the effects of a catalyst pre-treatment on the activity and stability of the same catalysts, and compared their behaviour to pure Pd. The aim of the present study is to investigate the catalytic properties of a series of catalysts composed of mixtures of platinum, palladium and rhodium, with an emphasis on their resistance to thermal and hydrothermal ageing. Hydrothermal ageing is essential for automotive exhaust applications, and thermal ageing is more relevant to fugitive emission combustion in the oil and gas industry. In addition to the study of catalysts not reported earlier, we have extended the work to include thermal ageing and the effects of ageing temperature.

This paper adds value to the literature in showing the results from the ageing of commercial catalysts. There is a lack of such data in the literature, and these results will be especially valuable for those wishing to compare their "in-house" formulations with several industry standards. Furthermore, we highlight the positive effect of the Pt addition, and the negative effect of the Rh addition. Furthermore, most ageing studies do not compare the relative effects of dry and wet ageing, which is of interest.

2. Materials and Methods

The experimental procedures used are described elsewhere [110,111], and the basic description is included here for completeness. Catalyst activity measurements were made using a small reactor system consisting of a reactor, furnace, thermocouples and temperature controller, flow meters, gas and water supply, as shown in Figure 1. The reactor had an inner tube of 0.76 cm (3/8″) diameter with an outer sleeve of 2.22 cm (7/8″) diameter, both made from 316 stainless steel. The role of the outer sleeve was to provide a constant temperature along the wall of the reactor. The reactor assembly was installed inside a tubular furnace. The catalyst was located in the middle of the reactor, and quartz wool was placed before and after the catalyst to contain the bed. Three thermocouples (K-type from Omega) were used to monitor the temperature in the reaction system. Thermocouples were placed in the inner tube of the reactor (before and after the catalyst sample), touching each end of the catalytic bed, as shown in Figure 1. The average of the temperatures recorded by these two thermocouples is reported as the reaction temperature. The maximum temperature difference between the two thermocouples was about five degrees. A thermocouple placed in the outer sleeve was used to control the reactor temperature via a PID controller on the reactor furnace.

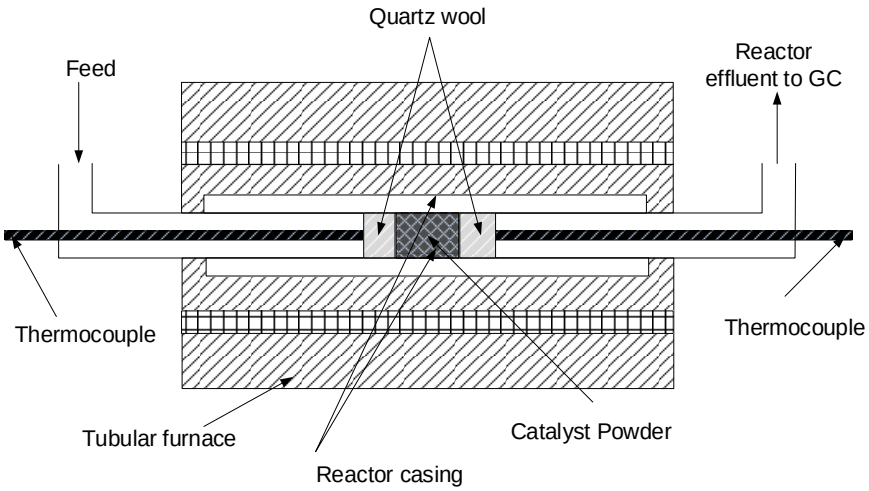

Figure 1. Schematic of the experimental reactor and furnace.

The reactor effluent was analysed with a gas chromatograph (GC HP-7890-A type from Agilent Technologies Incorporation, Santa Clara, CA, USA). The GC column was 19095 P-Q4. The carrier gas was helium (Ultra high purity 5.0 from Praxair, Danbury, CT, USA) with a flow rate of 11 cm^3/min.

The desired methane concentration was obtained by mixing 10 vol. % CH_4 in N_2 with extra dry air (Praxair). Methane and air flow rates were controlled by flow meters in separate lines (line 1 for extra dry air controlled by a Matheson Modular DYNA-blender model 8250 and line 2 for methane in the nitrogen mixture controlled by an MKS Type 1479). The gases were mixed before entering the reactor. For all experiments, the flow rate of air was 225 $\pm$ 1.5 cm^3/min, while the flow rate of methane balanced in nitrogen was 9.62 cm^3/min to obtain a concentration of 4100 ppm by volume. For the experiments with added water, 5 vol. % water vapour was added to the feed by the injection of liquid water from a syringe pump (KDS100L). The reactor feed line was heated to evaporate the water and to avoid condensation. All reported gas flow rates are based on 0 °C and 1 atm. The oxygen concentration was always about 20% by volume (plus or minus 0.3%) and thus represents a lean operation.

The experimental conditions and the temperature controller, GC and water syringe pump system were controlled by the LabView software connected to an Opto-22 system.

Catalyst samples were commercial products provided by Umicore AG in the form of washcoated 400 CPSI square channel monoliths. Seven catalysts were used in the investigation, containing various combinations of precious metals. In the following, the metal loadings are reported as g/ft^3 of PGM based on the monolith volume, prior to it being crushed. These loading levels are typical for catalytic converter applications for compression ignition engines fuelled by natural gas. The mass percent of the PGM in the catalyst samples was calculated assuming a monolith bulk density of 544.5 kg/m^3 and a washcoat density of 1100 kg/m^3. The washcoat was assumed to occupy 12% of the monolith volume, which is a typical value [111]. The catalyst compositions are summarized in Table 1. In addition to the PGM loading in the monolith, the estimated mass percent of PGM in the washcoat is also given, to better to compare with literature results.

Table 1. Precious metals loadings of the seven catalysts studied in this investigation. The number in the catalyst designation gives the total PGM loading on the monolith.

	PGM Loading on Monolith g/ft^3			**Mass % PGM in Washcoat**		
Designation	Pt	Pd	Rh	Pt	Pd	Rh
Pt 95	95			2.54		
Pt:Pd 95	76	19		2.03	0.51	
Pd 150		150			4.01	
Pt:Pd 150	25	125		0.67	3.34	
Pd 122		122			3.26	
Pd:Rh 120		117.15	2.85		3.13	0.076
Pt:Pd:Rh 95	19	73	2.85	0.51	1.95	0.076

The monoliths were crushed, ground and screened using sieves to form particles in the range of 300–400 microns. Approximately 66% by mass of the reactor charge is Cordierite, which serves to dilute the bed and to preserve a more uniform temperature. The total catalyst charge was 0.5 g to give a GHSV of 27 100 h^{-1}.

Catalysts Pt 95 and Pt:Pd 95 were Diesel oxidation catalysts, and had been de-greened at 650 °C for 16 h prior to receipt. Although these catalysts were not specifically designed for the combustion of methane, they were included for completeness, and also because we had previously studied these catalysts to some extent for methane combustion [110,111]. The other catalysts were designed as methane combustion catalysts, and were provided without any pre-treatment and were de-greened under flowing air either at 650 °C or 550 °C, depending on the experiments. That is, the de-greening was conducted at 550 °C when

the subsequent ageing was to be performed at this temperature, and at 650 °C for ageing studies at the higher temperature. Because catalysts Pt 95 and Pt:Pd 95 were previously exposed to 650 °C, few ageing experiments were conducted at 550 °C for these two catalysts. The de-greening of the supported catalyst was performed to obtain a more stable structure as well as to remove any volatiles remaining from the synthesis process.

To have the same base line in the experiments, all of the catalyst samples were reduced prior to use. Hydrogen was fed to the reactor at 50 cm^3/min, then the temperature of the reactor was raised at 500 °C and held there for 30 min. The hydrogen flow was stopped and nitrogen was fed to the reactor at 50 cm^3/min. The reactor was slowly brought to room temperature, then nitrogen flow was cut off and air was fed to the reactor overnight at 50 cm^3/min. In [112], it was reported that for palladium-based catalysts, the reduction step resulted in an increase in activity compared to the unreduced sample. However, the increased activity rapidly disappeared after heating in an oxidizing atmosphere.

We report three types of tests. The catalyst activity was measured over the temperature range of interest. In these tests, the temperature was increased stepwise, with the temperature being held constant for at least one hour at each temperature level. Several gas analyses were performed at each temperature. The temperature was raised in steps of 40 or 50 °C up to the maximum, which was either 550 or 650 °C. The reactor was then cooled stepwise in a similar manner, and the activity measured at several points during the process to obtain extinction curves. The catalyst activities are reported here based on the extinction curves. Note that the temperature was never raised higher than the ageing temperature during the activity tests, and thus in some cases 100% conversion was not observed.

The second test set performed were thermal ageing tests. In these experiments, the catalyst sample was held at the ageing temperature, usually either 550 or 650 °C, for an extended period of time. The temperature was periodically reduced to a specified temperature to measure the activity for methane conversion, and thus to follow the progress of the deactivation, and then returned to the higher value. The third set of tests involved hydrothermal ageing. These experiments were performed in the same manner as the thermal ageing ones, except that 5% by volume water was added to the feed. See Section 3 for more details on the thermal and hydrothermal ageing protocols.

3. Results

This section presents the results achieved from the thermal and hydrothermal ageing studies. Four of the catalysts were tested using de-greening and ageing temperatures of 650 °C. The four catalysts used were Pt 95, Pt:Pd 95, Pd 150 and Pt:Pd 150. Five of the catalysts were first tested using de-greening and ageing temperatures of 550 °C. The five catalysts used were Pd 150, Pd 122, Pt:Pd 150, Pd:Rh 120 and Pt:Pd:Rh 95.

Figures 2–9 show the activity curves for all of the seven catalysts for the fresh, thermally aged (TA) and hydrothermally aged (HTA) cases.

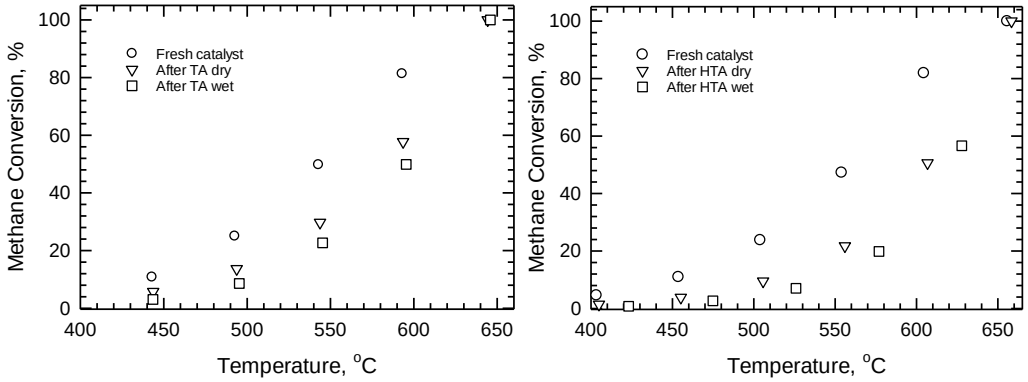

Figure 2. Activities of fresh and aged catalysts. Pt 95 catalyst with ageing at 650 °C.

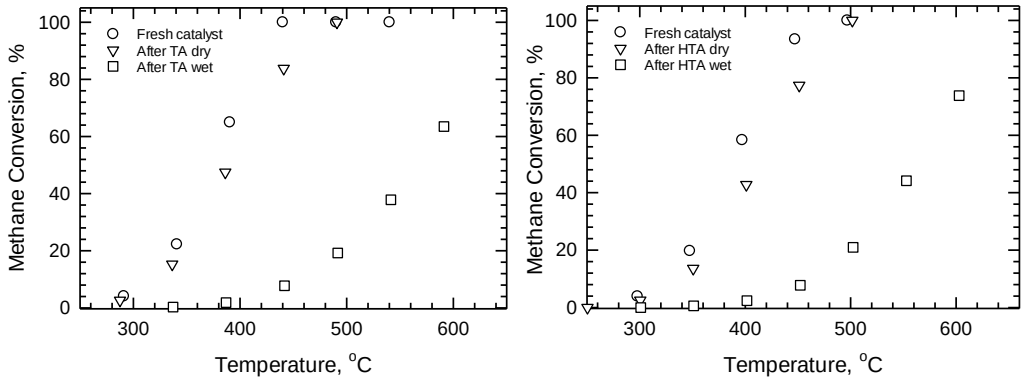

Figure 3. Activities of fresh and aged catalysts. Pt:Pd 95 catalyst with ageing at 650 °C.

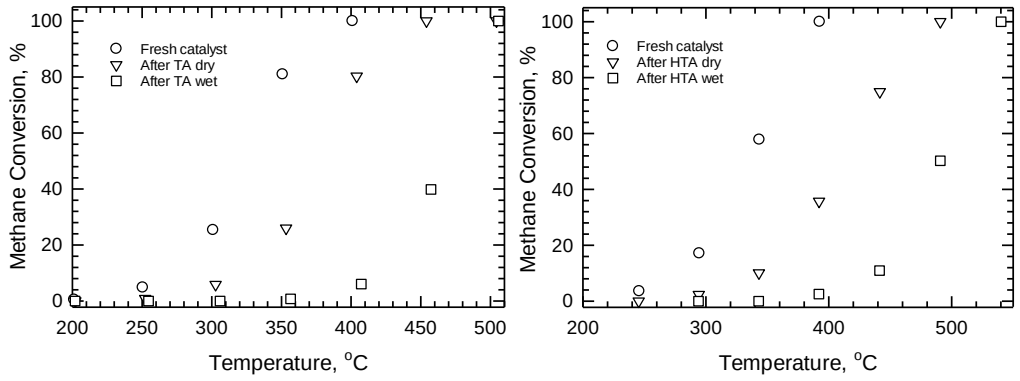

Figure 4. Activities of fresh and aged catalysts. Pd 150 catalyst with ageing at 550 °C.

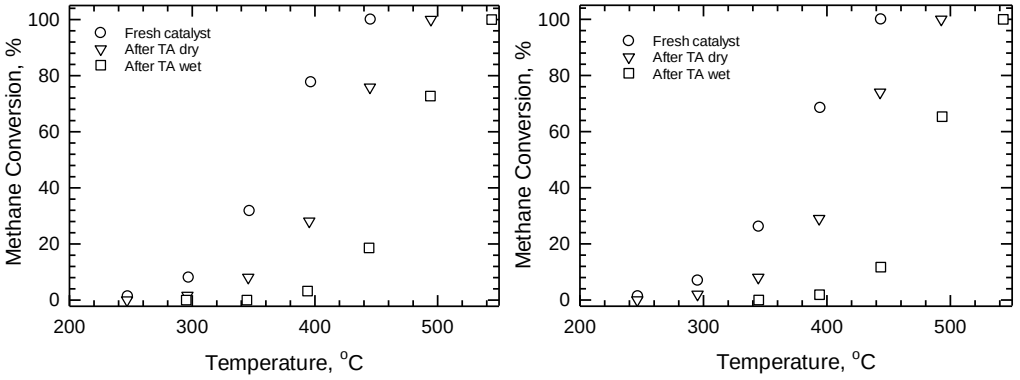

Figure 5. Activities of fresh and aged catalysts. Pd 122 catalyst with ageing at 550 °C.

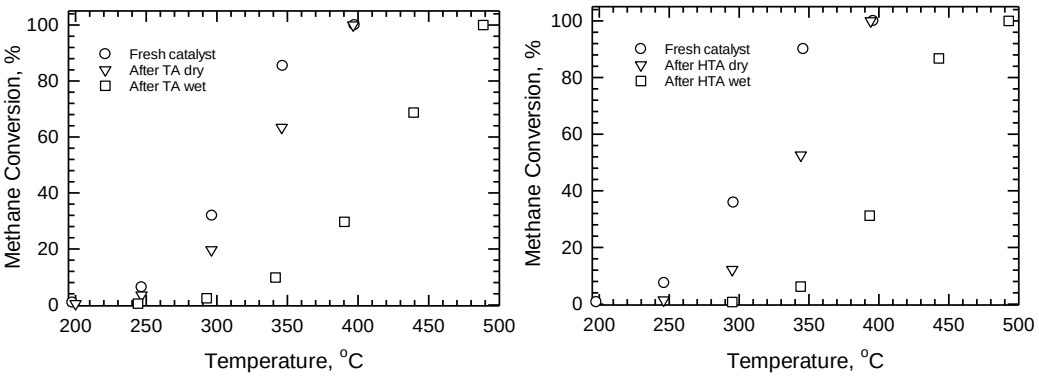

Figure 6. Activities of fresh and aged catalysts. Pt:Pd 150 catalyst with ageing at 550 °C.

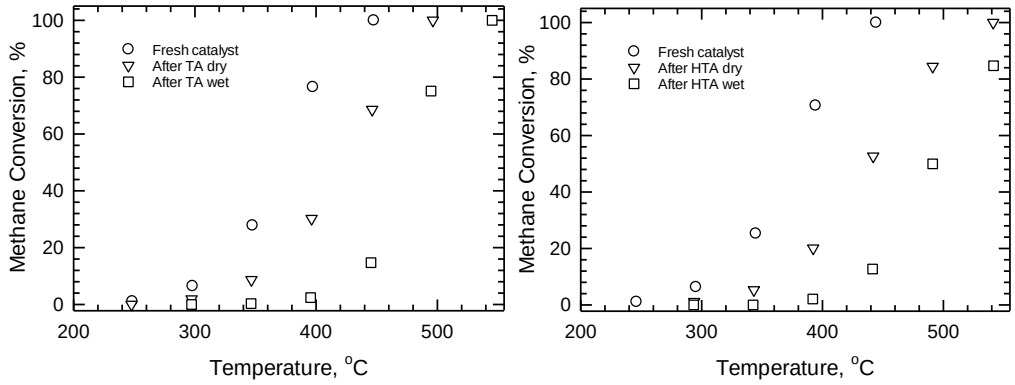

Figure 7. Activities of fresh and aged catalysts. Pd:Rh 120 catalyst with ageing at 550 °C.

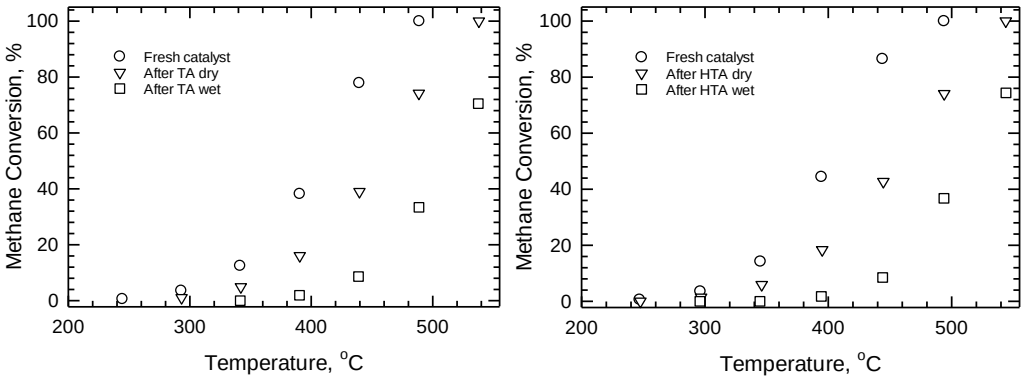

Figure 8. Activities of fresh and aged catalysts. Pt:Pd:Rh 95 catalyst with ageing at 550 °C.

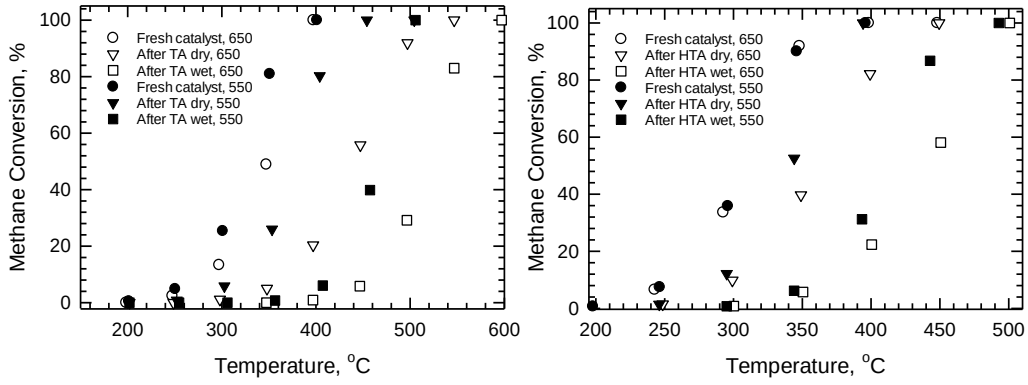

Figure 9. Comparisons of activities after ageing at different temperatures. (**Left**): Pd 150 catalyst with thermal aging at 550 °C and 650 °C. (**Right**): Pt:Pd 150 catalyst with hydrothermal ageing at 550 °C and 650 °C.

Note that each conversion point on the graphs, and the values given in the following tables, represents the average of four measurements taken at each temperature. We also note that the ageing experiments on each catalyst were repeated, often several times, and very good repeatability was observed. A typical example of the repeatability is shown at the end of this section.

From the activity plots, it is evident that TA and HTA both cause a loss in activity over time, as expected, and that the presence of water has an inhibition effect. Considering Figure 9, it is also observed that the ageing temperature also affects the activity, with a higher ageing temperature causing greater activity loss. To quantify the activity loss and the inhibition effect, it is convenient to present a table of results that represent the temperature required to achieve benchmark conversions, which are often set at 25, 50 and 75% conversion levels. The values at these three conversion benchmarks were calculated

using linear interpolation between the closest measured conversions. The temperature required to achieve a 50% conversion is often referred to in the literature as the "light-off" temperature, although care has to be taken with its use, as the value obviously depends on the operating conditions, especially the feed flow rate.

Table 2 presents a table of the temperature increase required, compared to the fresh catalyst activity in the absence of added water, to achieve 50% conversion after TA and HTA, both in the presence and absence of added water. As can be observed from this table, the Pt 95 catalyst had the smallest difference in the presence of water. Table 3 then gives the temperature values for the seven catalysts of the three conversion benchmarks. The activity results are discussed more fully in Section 4. Note that a different catalyst sample was used for each TA and HTA test; therefore, there is some difference in the fresh catalyst activity in each case, as a result of the usual sample-to-sample variation.

Table 2. Temperature increase needed to obtain 50% conversion after TA and HTA for the seven catalysts investigated. Pt 95 and Pt:Pd 95 were aged at 650 °C, and the others at 550 °C.

Catalyst	TA Dry	TA Wet	HTA Dry	HTA Wet
Pt 95	37	53	48	61
Pt:Pd 95	17	192	26	177
Pd 150	53	143	74	157
Pt:Pd 150	18	103	32	101
Pd 122	51	106	44	106
Pd:Rh 120	52	104	66	119
Pt:Pd:Rh 95	50	106	55	111

The activity of each catalyst after the different ageing treatments provides much useful information. We now demonstrate the activity behaviour during the ageing. The ageing protocols were as follows. The temperature was held at either 550 or 650 °C for two hours, and then the temperature was lowered to measure the conversion at either 350 or 450 °C (or, only for the Pt 95 catalyst, 550 °C). Four measurements of the effluent composition were made over a one-hour period, and then the temperature was raised to the ageing temperature. The cycling was repeated, and then at 22 h it was stopped and the catalyst held at the same temperature was used to record the activity. For the TA experiments, 5% water was then added to the feed at a total elapsed time of 30 h. After 33 h of time, the water in the feed was stopped, for both TA and HTA, and the experiment continued for about 10 h more. The reactor was then cooled under flowing air.

Figure 10 shows the activity during aging for the Pt 95 catalyst. For both TA and HTA, the ageing was conducted at 650 °C and the activity measured at 550 °C. Each data point represents the average of four measurements, all of which appeared to be randomly distributed with a range of 1 °C.

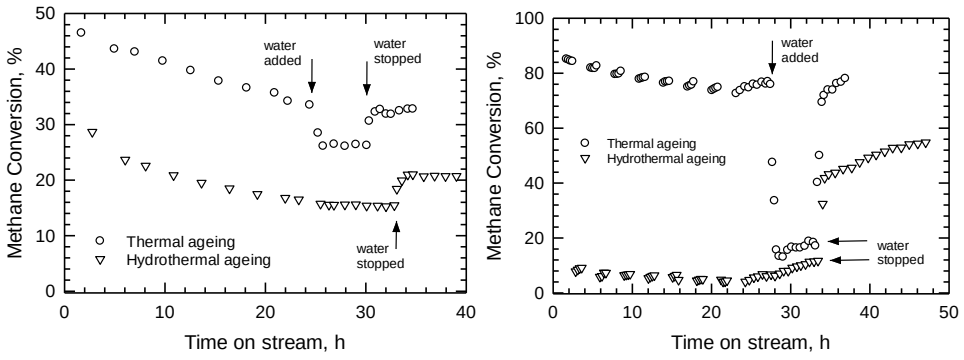

Figure 10. Activity during ageing studies. (**Left**): Pt 95 catalyst with ageing at 650 °C and activity measured at 550 °C. (**Right**): Pt:Pd 95 catalyst with aging at 650 °C and activity measured at 450 °C.

Table 3. Temperatures required to achieve 25, 50 and 75% conversion.

Pt 95 catalyst aged at 650 °C						
Conversion	Fresh	TA dry	TA wet	Fresh	HTA dry	HTA wet
25	493	529	550	506	562	584
50	543	580	596	558	606	619
75	583	614	621	595	632	650
Pt:Pd 95 catalyst aged at 650 °C						
Conversion	Fresh	TA dry	TA wet	Fresh	HTA dry	HTA wet
25	344	351	507	354	370	511
50	373	390	565	386	412	563
75	405	428	608	421	448	608
Pd 150 catalyst aged at 550 °C						
Conversion	Fresh	TA dry	TA wet	Fresh	HTA dry	HTA wet
25	301	353	435	304	372	459
50	323	376	466	334	410	491
75	345	399	486	363	442	515
Pd 122 catalyst aged at 550 °C						
Conversion	Fresh	TA dry	TA wet	Fresh	HTA dry	HTA wet
25	333	388	450	342	389	456
50	367	418	473	373	417	479
75	394	444	498	405	445	507
Pt:Pd 150 catalyst aged at 550 °C						
Conversion	Fresh	TA dry	TA wet	Fresh	HTA dry	HTA wet
25	283	302	379	277	311	381
50	313	331	416	309	341	410
75	337	362	449	332	368	432
Pd:Rh 120 catalyst aged at 550 °C						
Conversion	Fresh	TA dry	TA wet	Fresh	HTA dry	HTA wet
25	345	387	454	345	400	458
50	370	422	474	372	438	491
75	396	456	495	402	477	527
Pt:Pd:Rh 95 catalyst aged at 550 °C						
Conversion	Fresh	TA dry	TA wet	Fresh	HTA dry	HTA wet
25	365	410	472	363	409	473
50	405	455	511	401	456	512
75	436	489	543	430	496	545

Figure 10 also shows the activity decline for the Pt:Pd 95 catalyst. The activities were measured at 450 °C. Significant differences were observed compared to the Pt 95 catalyst. The same protocol of taking four measurements at 450 °C was followed. In this case, however, we show all four of the points, because there appears to be a trend of an increase in activity (albeit small) over the one-hour period. After 22 h of TA, when the temperature was then held constant at 450 °C, there is a marked recovery in activity. The addition of water causes a very large drop in conversion, which is then largely recovered when the water was switched off. The same behaviour was observed for HTA, with a small but noticeable recovery in activity at 450 °C, and then a significant recovery in activity when the water flow was terminated.

Next, we present the results for the two catalysts containing only palladium, Pd 150 and Pd 122. Figure 11 shows the results of TA and HTA with ageing at 550 °C for catalyst Pd

150. The activity was measured at either 350 °C (TA) or 450 °C (HTA). Four measurements of effluent concentrations were made over an approximately one-hour period.

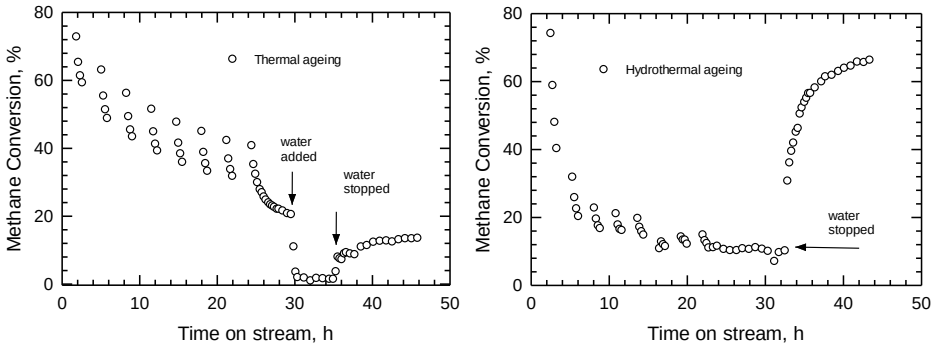

Figure 11. Activity during ageing studies of Pd 150 catalyst at 550 °C. (**Left**): Thermal ageing with activity measured at 350 °C. (**Right**): Hydrothermal ageing with activity measured at 450 °C.

Figure 12 shows the results of TA and HTA for the Pd 122 catalyst, with 550 °C ageing and activity measured at 450 °C. Similar trends to the Pd 150 catalyst were observed.

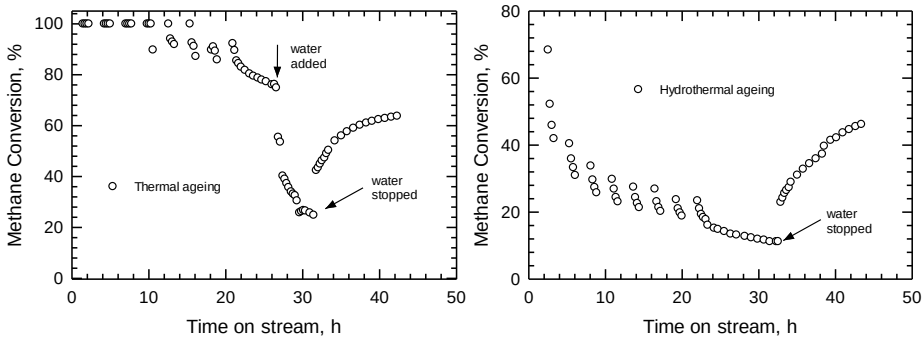

Figure 12. Activity during ageing studies of Pd 122 catalyst at 550 °C. (**Left**): Thermal ageing with activity measured at 450 °C. (**Right**): Hydrothermal ageing with activity measured at 450 °C.

Figure 13 presents the ageing curves for the Pt:Pd catalyst for 550 °C ageing with activity measured at 350 °C, and also for 650 °C ageing with activity at 350 °C. In this case, it can be observed that the higher ageing activity results in more rapid catalyst deactivation, which is also observed in the activity plots of Figure 9.

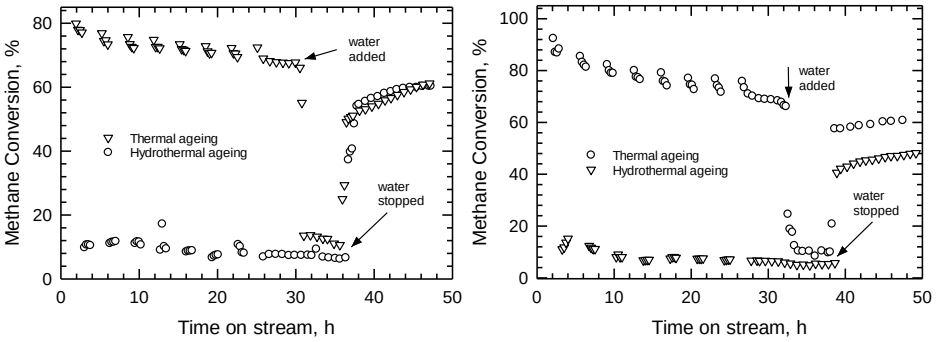

Figure 13. Activity during ageing studies of Pt:Pd 150 catalyst. (**Left**): Thermal and hydrothermal ageing at 550 °C with activity measured at 350 °C. (**Right**): Thermal and hydrothermal ageing at 650 °C with activity measured at 350 °C.

Figure 14 shows the results for the Pd:Rh 120 catalyst. In this case, for comparison purposes, the activity during TA was measured at both 350 and 450 °C. For HTA, the activity was recorded at 450 °C. As before, water is observed to cause a large reduction

in activity, which recovers after the water is switched off. In addition, there appears to be some activity recovery at each high temperature cycle.

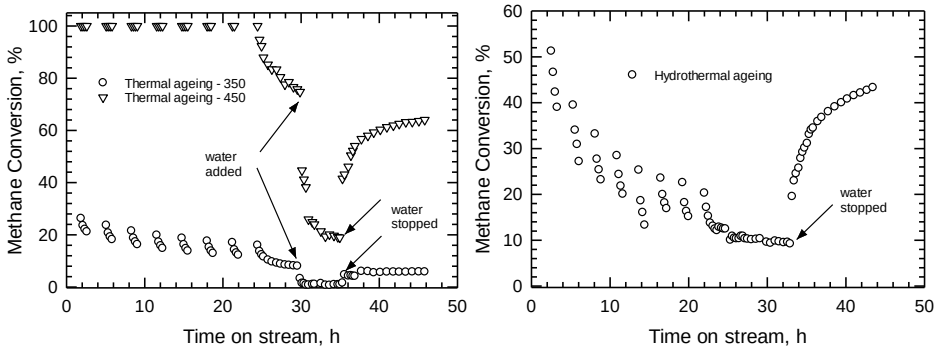

Figure 14. Activity during ageing studies of Pd:Rh 120 catalyst at 550 °C. (**Left**): Thermal ageing with activity measured at 350 °C and 450 °C. (**Right**): Hydrothermal ageing with activity measured at 450 °C.

The deactivation plots for the final catalyst, Pt:Pd:Rh 95, are given in Figure 15. The protocols were the same as the other catalysts, however, in this case there was a significant difference in the behaviour for the HTA. The activity at 550 °C fell below 100% during the ageing process, and therefore, for the HTA results, Figure 15 shows the activity at 550 °C as well as at 450 °C.

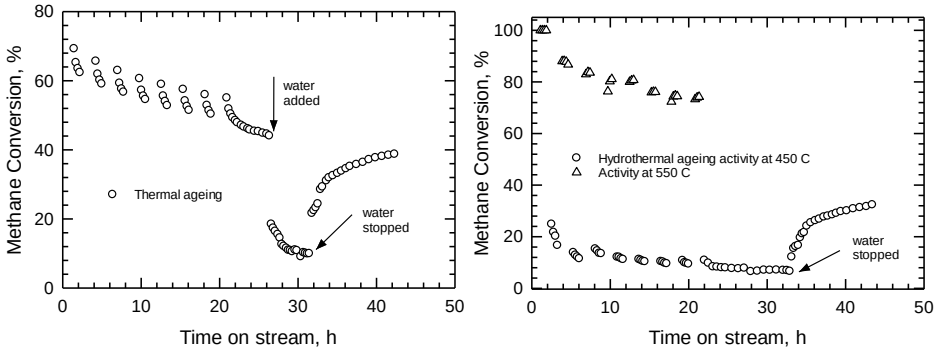

Figure 15. Activity during ageing studies of Pt:Pd:Rh 95 catalyst at 550 °C. (**Left**): Thermal ageing with activity at 450 °C. (**Right**): Hydrothermal ageing with activity at 450 °C.

As an example of the experimental repeatability, Figure 16 shows the repeatability of the HTA experiments for the Pt 95 catalyst carried out at 650 °C. The deactivation curves are similar. After ageing, both catalyst tests show a minimal inhibition effect by water.

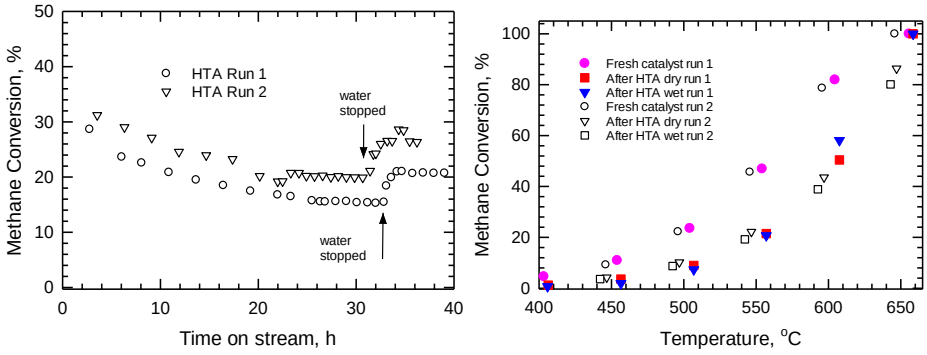

Figure 16. Comparison of two hydrothermal ageing runs for the Pt 95 catalyst. The ageing temperature was 650 °C. The ageing curves are presented on the (**left**) and the activity curves before and after ageing on the (**right**).

4. Discussion

Having presented the results, we provide some general discussion regarding their significance. Considering the research in methane catalysts that we have reported over the past few years, and the consensus in the literature, many of the trends observed are expected. The pure platinum catalyst, Pt 95, had the lowest overall activity, as expected for the fuel lean environment. It had the best relative resistance to deactivation in HTA, and the effect of water on the conversion for the fully hydrothermally aged catalyst is relatively small, compared to the other catalysts in the series.

Replacing a relatively small amount of the Pt by Pd, as is conducted for catalyst Pt:Pd 95, gave a quite dramatic increase in activity. On the other hand, this latter catalyst is very strongly inhibited by water, after either TA or HTA. The dry activity after TA or HTA was also reduced by a smaller amount compared to the pure Pt case, based on the temperature increase required to maintain a 50% conversion (see Table 2). The extreme sensitivity of the Pt:Pd catalyst to water can also be observed by comparing the deactivation plots. When water was added to the Pt:Pd catalyst during TA, the activity dropped to a value close to the conversion observed at the same time for the catalyst during HTA. Another interesting point was the behaviour of the catalyst during the ageing process. As mentioned earlier, for the Pt 95 catalyst, the measured activity for the four data points collected during the reduced temperature portion of the ageing curve was the same. That is, the conversion was essentially the same at each of the four points. For the Pt:Pd 95 case, the situation was different. The conversion for each of the four points demonstrated a small but noticeable increase over the one-hour period. Although small, it was a consistent trend.

The two Pd only catalysts behaved in a similar manner, with Pd 150 being more active than Pd 122, as expected. Both Pd-only catalysts showed a strong inhibition effect when water was present. Another result observed for both catalysts relates to the activity measured during the ageing process. Each time the temperature was lowered from 550 °C to the measurement temperature, four measurements were made. In each case, the four measurements demonstrated a systematic decline over the approximately one-hour measurement time. Furthermore, the first data point had a higher conversion than the last data point of the previous measurement cycle. Therefore, we observe that although there is a systematic decline in activity over the ageing period, it would appear that there is a recovery of some activity at each 550 °C portion of the cycle. This behaviour is observed for all of the catalysts that contained predominantly palladium. We also observed that, although the Pd 122 catalyst was less active in general than the Pd 150 one, it was less affected by water inhibition after both TA and HTA, as measured by the temperature increase required to achieve a 50% conversion, as shown in Table 2. We speculate that this effect might be the result of the increased sintering with HTA for the Pd 150 catalyst, as it is known that the sintering of Pd increases with Pd loading.

Overall, the most active catalyst was the Pt:Pd 150 catalyst. It had the highest overall activity, both in the fresh state and after TA and HTA. We have previously observed (for other catalysts) that a pure Pd catalyst is more active than at a Pt:Pd bimetallic catalyst for dry methane combustion [92]; however, in that case, all other variables of the catalyst composition were the same, making a direct comparison easier. The increase in reactor temperature required to achieve a 50% conversion after TA or HTA in the presence of water was, however, similar to the values obtained for the catalysts Pd 122, Pd:Rh 120 and Pt:Pd:Rh 95. We also note that ageing at a higher temperature (650 °C compared to 550 °C) gives a higher loss in catalyst activity.

The addition of Rh to the other PGM does not have a huge positive effect on the methane combustion activity. Indeed, for the catalyst Pt:Pd:Rh 95, the catalyst would not maintain 100% conversion at 550 °C throughout the HTA process.

We also comment on the effect of the water addition during TA. Water was added for a short period, which resulted in a quick drop in activity, as expected. After the water was terminated, the activity returned slowly to the value observed without water. For the

HTA process, at the end, when the water flow was terminated, the activity increases slowly, although in most cases not to the level of the catalyst exposed to a TA process.

We examined several of the catalysts before and after the ageing using transmission electron microscopy (TEM). Figure 17 shows the Pt 95 catalyst before and after HTA. Figure 18 shows the result for the Pt:Pd 95 catalyst before and after HTA, whilst Figure 19 shows the before and after HTA TEM pictures for the Pt:Pd 150 catalyst. An increase in particle size can be observed as a result of sintering in all cases.

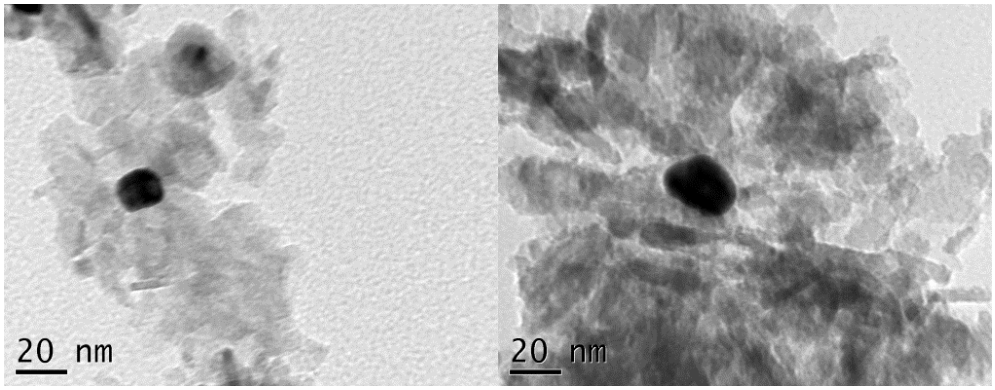

Figure 17. TEM images of Pt 95 catalyst before (**left**) and after (**right**) hydrothermal ageing.

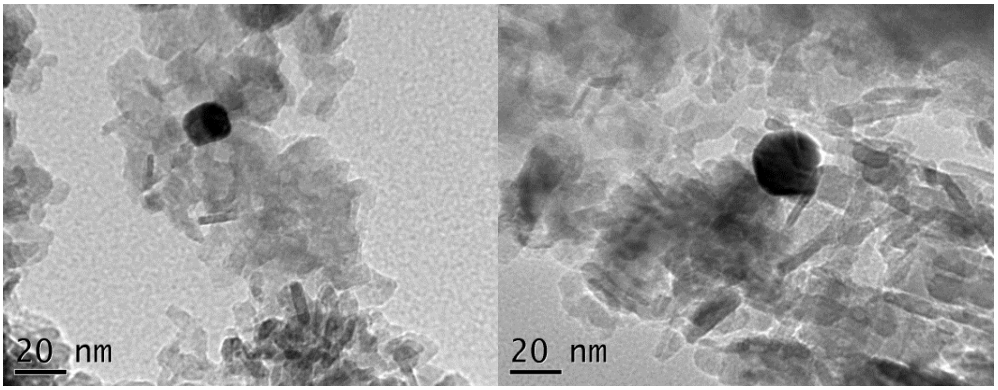

Figure 18. TEM images of Pt:Pd 95 catalyst before (**left**) and after (**right**) hydrothermal ageing.

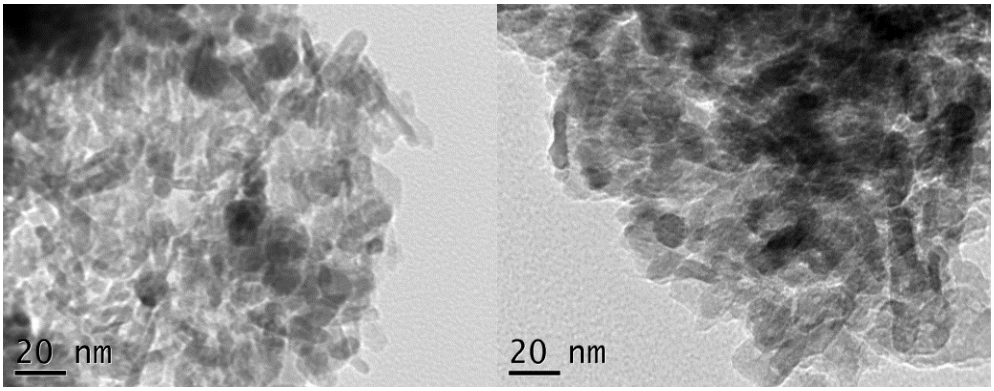

Figure 19. TEM images of Pt:Pd 150 catalyst before (**left**) and after (**right**) hydrothermal ageing.

5. Conclusions

We have studied the thermal and hydrothermal ageing of a series of PGM-based catalysts for the catalytic combustion of lean methane mixtures in the presence and absence of added water. The best catalyst tested was pre-dominantly palladium, with some platinum added. This catalyst demonstrated the highest overall activity, and the best resistance to

deactivation and inhibition by water. The addition of rhodium to the catalyst caused a more rapid deactivation. These tests on the commercial catalysts should provide a useful benchmark for other researchers in the area of the catalytic combustion of methane.

Author Contributions: Conceptualization, G.M.I. and R.E.H.; methodology, G.M.I. and R.E.H.; software, G.M.I.; formal analysis, G.M.I. and R.E.H.; investigation, G.M.I. and R.E.H.; resources, R.E.H.; data curation, G.M.I. and R.E.H.; writing—original draft preparation, R.E.H.; writing—review and editing, G.M.I.; visualization, G.M.I. and R.E.H.; supervision, R.E.H.; project administration, R.E.H.; funding acquisition, R.E.H. All authors have read and agreed to the published version of the manuscript.

Funding: This research was funded by the Natural Science and Engineering Research Council of Canada (NSERC) G.M. Istratescu acknowledges scholarships from the NSERC and Alberta Ingenuity.

Data Availability Statement: The data presented in this study may be available on request from the corresponding author. The data are not publicly available.

Conflicts of Interest: The authors declare no conflict of interest. The funders had no role in the design of the study; in the collection, analyses, or interpretation of data; in the writing of the manuscript; or in the decision to publish the results.

References

1. Kesselring, J. Catalytic combustion. In *Advanced Combustion Methods*; Weinberg, J., Ed.; Academic Press: London, UK; pp. 237–275.
2. Prasad, R.; Kennedy, L.; Ruckenstein, E. Catalytic combustion. *Catal. Rev. Sci. Eng.* **1984**, *29*, 219–267. [CrossRef]
3. Hayes, R.E.; Kolaczkowski, S.T. *Introduction to Catalytic Combustion*; Gordon and Breach Science Publishers: Reading, UK, 1997.
4. Ismagilov, Z.; Kerzhentsev, M. Catalytic fuel combustion—A way of reducing emission of nitrogen oxides. *Catal. Rev. Sci. Eng.* **1990**, *32*, 51–103. [CrossRef]
5. Sadamori, H. Application concepts and evaluation of small-scale catalytic combustors for natural gas. *Catal. Today* **1999**, *47*, 325–338. [CrossRef]
6. Etemad, S.; Karim, H.; Smith, L.; Pfefferle, W. Advanced technology catalytic combustor for high temperature ground power gas turbine applications. *Catal. Today* **1999**, *47*, 305–313. [CrossRef]
7. Forzatti, P. Status and perspectives of catalytic combustion for gas turbines. *Catal. Today* **2003**, *83*, 3–188. [CrossRef]
8. Hayes, R.E. Catalytic solutions for fugitive methane emissions in the oil and gas sector. *Chem. Eng. Sci.* **2004**, *59*, 4073–4080. [CrossRef]
9. Zanoletti, M.; Klvana, D.; Kirchnerova, J.; Perrier, M.; Guy, C. Auto-cyclic reactor: Design and evaluation for the removal of unburned methane from emissions of natural gas engines. *Chem. Eng. Sci.* **2009**, *64*, 945–954. [CrossRef]
10. Kolios, G.; Gritsch, A.; Morillo, A.; Tuttlies, U.; Bernnat, J.; Opferkuch, F.; Eigenberger, G. Heat-integrated reactor concepts for catalytic reforming and automotive exhaust purification. *Appl. Catal. B Environ.* **2007**, *70*, 16–30. [CrossRef]
11. Bernnat, J.; Rink, M.; Tuttlies, U.; Danner, T.; Nieken, U.; Eigenberger, G. Heat-integrated concepts for automotive exhaust purification. *Top. Catal.* **2009**, *52*, 2052–2057. [CrossRef]
12. Chen, J.; Arandiyan, H.; Gao, X.; Li, J. Recent advances in catalysts for methane combustion. *Catal. Surv. Asia* **2015**, *19*, 140–171. [CrossRef]
13. Cimino, S.; Di Benedetto, A.; Pirone, R.; Russo, G. Transient behaviour of perovskite-based monolithic reactors in the catalytic combustion of methane. *Catal. Today* **2001**, *69*, 95–103. [CrossRef]
14. Park, S.; Hwang, H.; Moon, J. Catalytic combustion of methane over rare earth stannate pyrochlore. *Catal. Lett.* **2003**, *87*, 219–223. [CrossRef]
15. Feng, S.; Wang, Z.; Yang, P. Effect of Substitution of Cobalt for Iron in Sr4Fe6O13-delta on the Catalytic Activity for Methane Combustion. *Chin. J. Chem.* **2011**, *29*, 451–454. [CrossRef]
16. Yang, J.; Guo, Y. Nanostructured perovskite oxides as promising substitutes of noble metals catalysts for catalytic combustion of methane. *Chin. Chem. Lett.* **2018**, *29*, 252–260. [CrossRef]
17. Zhu, W.; Jin, J.; Chen, X.; Li, C.; Wang, T.; Tsang, C.; Liang, C. Enhanced activity and stability of La-doped CeO2 monolithic catalysts for lean-oxygen methane combustion. *Environ. Sci. Pollut. Res.* **2018**, *25*, 5643–5654. [CrossRef]
18. Li, S.; Zhang, Y.; Wang, Z.; Du, W.; Zhu, G. Morphological effect of CeO2 catalysts on their catalytic performance in lean methane combustion. *Chem. Lett.* **2020**, *49*, 461–464. [CrossRef]
19. Chen, J.; Zhang, X.; Arandiyan, H.; Peng, Y.; Chang, H.; Li, J. Low temperature complete combustion of methane over cobalt chromium oxides catalysts. *Catal. Today* **2013**, *201*, 12–18. [CrossRef]
20. Choya, A.; de Rivas, B.; González-Velasco, J.; Gutiérrez-Ortiz, J.; López-Fonseca, R. Oxidation of residual methane from VNG vehicles over Co3O4-based catalysts: Comparison among bulk, Al2O3-supported and Ce-doped catalysts. *Appl. Catal. B Environ.* **2018**, *237*, 844–854. [CrossRef]

21. Liotta, L.; Di Carlo, G.; Pantaleo, G.; Deganello, G. Co3O4/CeO2 and Co3O4/CeO2–ZrO2 composite catalysts for methane combustion: Correlation between morphology reduction properties and catalytic activity. *Catal. Commun.* **2005**, *6*, 329–336. [CrossRef]
22. Cullis, C.F.; Willatt, B.M. Oxidation of methane over supported precious metal catalysts. *J. Catal.* **1983**, *83*, 267–285. [CrossRef]
23. Gélin, P.; Primet, M. Complete oxidation of methane at low temperature over noble metal based catalysts: A review. *App. Cat. B Environ.* **2002**, *39*, 1–37. [CrossRef]
24. Choudhary, T.; Banerjee, S.; Choudhary, V. Catalysts for combustion of methane and lower alkanes. *Appl. Catal. A Gen.* **2002**, *234*, 1–23. [CrossRef]
25. Ciuparu, D.; Lyubovsky, M.; Altman, E.; Pfefferle, L.; Datye, A. Catalytic combustion of methane over palladium-based catalysts. *Catal. Rev. Sci. Eng.* **2002**, *44*, 593–649. [CrossRef]
26. Monai, M.; Montini, T.; Gorte, R.; Fornasiero, P. Catalytic Oxidation of Methane: Pd and Beyond. *Eur. J. Inorg. Chem.* **2018**, *25*, 2884–2893. [CrossRef]
27. Becker, E.; Carlsson, P.A.; Grönbeck, H.; Skoglundh, M. Methane oxidation over alumina supported platinum investigated by time-resolved in situ XANES spectroscopy. *J. Catal.* **2007**, *252*, 11–17. [CrossRef]
28. Deutschmann, O.; Maier, L.; Riedel, U.; Stroemman, A.; Dibble, R. Hydrogen assisted catalytic combustion of methane on platinum. *Catal. Today* **2000**, *59*, 141–150. [CrossRef]
29. Bui, P.; Vlachos, D.; Westmoreland, P. Catalytic ignition of methane/oxygen mixtures over platinum surfaces: Comparison of detailed simulations and experiments. *Surf. Sci.* **1997**, *385*, L1029–L1034. [CrossRef]
30. Deutschmann, O.; Behrendt, F.; Warnatz, J. Modeling and simulation of heterogeneous oxidation of methane on a platinum foil. *Catal. Today* **1994**, *21*, 461–470. [CrossRef]
31. Reinke, M.; Mantzaras, J.; Bombach, R.; Schenker, S.; Yylli, N. Effects of H_2O and CO_2 Dilution on the Catalytic and Gas-Phase Combustion of Methane, over Platinum at Elevated Pressures. *Combust. Sci. Tech* **2006**, *179*, 553–600. [CrossRef]
32. Mazzarino, I.; Barresi, A. Catalytic combustion of VOC mixtures in a monolith reactor. *Catal. Today* **1993**, *17*, 335–348. [CrossRef]
33. Niwa, M.; Awano, K.; Murakami, Y. Activity of supported platinum catalysts for methane oxidation. *Appl. Catal.* **1983**, *7*, 317–325. [CrossRef]
34. O'Connell, M.; Kolb, G.; Zapf, R.; Men, Y.; Hessel, V. Bimetallic catalysts for the catalytic combustion of methane using microreactor technology. *Catal. Today* **2009**, *144*, 306–311. [CrossRef]
35. Trimm, D.; Lam, C. The combustion of methane on platinum-alumina fibre catalysts I Kinetics and Mechanism. *Chem. Eng. Sci.* **1980**, *35*, 1405–1413. [CrossRef]
36. Jodeiri, N.; Wu, L.; Mmbaga, J.; Hayes, R.E.; Wanke, S.E. Catalytic Combustion of VOC in a Counter-diffusive Reactor. *Catal. Today* **2010**, *155*, 147–153. [CrossRef]
37. Cullis, C.; Nevell, T.; Trimm, D. Role of the catalyst support in the oxidation of methane over palladium. *J. Chem. Soc. Faraday Trans. 1 Phys. Chem. Condens. Phases* **1972**, *68*, 1406–1412. [CrossRef]
38. Schwartz, W.; Ciuparu, D.; Pfefferle, L. Combustion of methane over palladium-based catalysts: Catalytic deactivation and role of the Support. *J. Phys. Chem. C* **2012**, *116*, 8587–8593. [CrossRef]
39. Schwartz, W.; Pfefferle, L.D. Combustion of methane over palladium-based catalysts: Support interactions. *J. Phys. Chem. C* **2012**, *116*, 8571–8578. [CrossRef]
40. Escandon, L.; Ordonez, S.; Vega, A.; Diez, F. Oxidation of methane over palladium catalysts: Effect of the support. *Chemosphere* **2005**, *58*, 9–17. [CrossRef]
41. Kumar, R.; Hayes, R.; Semagina, N. Effect of support on Pd-catalyzed methane-lean combustion in the presence of water: Review. *Catal. Today* **2021**, *382*, 82–95. [CrossRef]
42. Garbowski, E.; Feumi-Jantou, C.; Mouaddib, N.; Primet, M. Catalytic combustion of methane over palladium supported on alumina catalysts: Evidence for reconstruction of particles. *Appl. Catal. A Gen.* **1994**, *109*, 277–292. [CrossRef]
43. Friberg, I.; Sadokhina, N.; Olsson, L. Complete methane oxidation over Ba modified Pd/Al2O3: The effect of water vapour. *Appl. Catal. B Environ.* **2018**, *231*, 242–250. [CrossRef]
44. Demoulin, O.; Navez, M.; Ruiz, P. Investigation of the behavior of a Pd/γ-Al_2O_3 catalyst during methane combustion reaction using in situ DRIFT spectroscopy. *Appl. Catal. A Gen.* **2005**, *295*, 59–70. [CrossRef]
45. Demoulin, O.; Navez, M.; Gaigneaux, E.; Ruiz, P.; Mamede, A.; Granger, P.; Payen, E. Operando resonance Raman spectroscopic characterisation of the oxidation state of palladium in Pd/g-Al_2O_3 catalysts during the combustion of methane. *Phys. Chem. Chem. Phys.* **2003**, *5*, 4394–4401. [CrossRef]
46. Datye, A.; Bravo, J.; Nelson, T.; Atanasova, P.; Lyubovsky, M.; Pfefferle, L. Catalyst microstructure and methane oxidation reactivity during the Pd-PdO transformation on alumina supports. *Appl. Catal. A Gen.* **2000**, *198*, 179–196. [CrossRef]
47. Ciuparu, D.; Perkins, E.; Pfefferle, L. In situ DR-FTIR investigation of surface hydroxyls on γ-Al_2O_3 supported PdO catalysts during methane combustion. *Appl. Catal. A Gen.* **2004**, *263*, 145–153. [CrossRef]
48. Castellazzi, P.; Groppi, G.; Forzatti, P.; Baylet, A.; Marecot, P.; Duprez, D. Role of Pd loading and dispersion on redox behaviour and CH_4 combustion activity of Al_2O_3 supported catalysts. *Catal. Today* **2010**, *155*, 18–26. [CrossRef]
49. Hicks, R.; Qi, H.; Young, M.; Lee, R. Effect of catalyst structure on methane oxidation over palladium on alumina. *J. Catal.* **1990**, *122*, 295–306. [CrossRef]

50. Hong, E.; Kim, C.; Lim, D.; Cho, H.; Shin, C. Catalytic methane combustion over Pd/ZrO2 catalysts: Effects of crystalline structure and textural properties. *Appl. Catal. B Environ.* **2018**, *232*, 544–552. [CrossRef]
51. Guerrero, S.; Araya, P.; Wolf, E. Methane oxidation on Pd supported on high area zirconia catalysts. *Appl. Catal. A Gen.* **2006**, *298*, 243–253. [CrossRef]
52. Fujimoto, F.; Ribiero, R.; Avalos Borja, A.; Iglesia, E. Structure and reactivity of PdO_x/ZrO_2 catalysts for methane oxidation at low temperatures. *J. Catal.* **1998**, *179*, 431–442. [CrossRef]
53. Carstens, J.; Su, S.; Bell, A. Factors Affecting the Catalytic Activity of Pd/ZrO2 for the Combustion of Methane. *J. Catal.* **1998**, *176*, 136–142. [CrossRef]
54. Ibashi, W.; Groppi, G.; Forzatti, P. Kinetic measurement of CH_4 combustion over a 10% PdO/ZrO_2 catalyst using an annular flow micro reactor. *Catal. Today* **2003**, *83*, 115–129. [CrossRef]
55. Araya, P.; Guerrero, S.; Robertson, J.; Gracia, F. Methane combustion over Pd/SiO_2 catalysts with different degrees of hydrophobicity. *Appl. Catal. A Gen.* **2005**, *283*, 225–233. [CrossRef]
56. Bassil, J.; Al Barazi, A.; Da Costa, P.; Boutros, M. Catalytic combustion of methane over mesoporous silica supported palladium. *Catal. Today* **2011**, *176*, 36–40. [CrossRef]
57. Hoyos, L.; Praliaud, H.; Primet, M. Catalytic combustion of methane over palladium supported on alumina and silica in presence of hydrogen sulfide. *Appl. Catal. A Gen.* **1993**, *98*, 125–138. [CrossRef]
58. Gannouni, A.; Albela, B.; Said Zina, M.; Bonneviot, L. Metal dispersion, accessibility and catalytic activity in methane oxidation of mesoporous templated aluminosilica supported palladium. *Appl. Catal. A Gen.* **2013**, *464–465*, 116–127. [CrossRef]
59. Ercolino, G.; Grzybek, G.; Stelmachowski, P.; Specchia, S.; Kotarba, A.; Specchia, V. Pd/Co3O4-based catalysts prepared by solution combustion synthesis for residual methane oxidation in lean conditions. *Catal. Today* **2015**, *257*, 66–71. [CrossRef]
60. Li, Z.; Xu, G.; Hoflund, G. In situ IR studies on the mechanism of methane oxidation over Pd/Al_2O_3 and Pd/Co_3O_4 catalysts. *Fuel Process. Technol.* **2003**, *84*, 1–11. [CrossRef]
61. Hoffmann, M.; Kreft, S.; Georgi, G.; Fulda, G.; Pohla, M.; Seeburg, D.; Berger-Karin, C.; Kondratenko, E.; Wohlrab, S. Improved catalytic methane combustion of Pd/CeO_2 catalysts via porous glass integration. *Appl. Catal. B Environ.* **2015**, *179*, 313–320. [CrossRef]
62. Lei, Y.; Li, W.; Liu, Q.; Lin, Q.; Zhenga, X.; Huanga, Q.; Guan, S.; Wanga, X.; Wang, C.; Li, F. Typical crystal face effects of different morphology ceria on the activity of Pd/CeO_2 catalysts for lean methane combustion. *Fuel* **2018**, *233*, 10–20. [CrossRef]
63. Huang, Q.; Li, W.; Lei, Y.; Guan, S.; Zheng, X.; Pan, Y.; Wen, W.; Zhu, J.; Zhang, H.; Lin, Q. Catalytic Performance of Novel Hierarchical Porous Flower-Like $NiCo_2O_4$ Supported Pd in Lean Methane Oxidation. *Catal. Lett.* **2018**, *148*, 2799–2811. [CrossRef]
64. Roth, D.; Gelin, P.; Tena, E.; Primet, M. Combustion of methane at low temperature over Pd and Pt catalysts supported on Al_2O_3, SnO_2 and Al_2O_3-grafted SnO_2. *Top. Catal.* **2001**, *16/17*, 77–82. [CrossRef]
65. Urfels, L.; Gelin, P.; Primet, M.; Tena, E. Complete oxidation of methane at low temperature over Pt catalysts supported on high surface area SnO_2. *Top. Catal.* **2004**, *30/31*, 427–432. [CrossRef]
66. Kinnunen, N.; Suvanto, M.; Moreno, M.; Savimaki, A.; Kallinen, K.; Kinnunen, T.; Pakkanen, T. Methane oxidation on alumina supported palladium catalysts: Effect of Pd precursor and solvent. *Appl. Catal. A Gen.* **2009**, *370*, 78–87. [CrossRef]
67. Lu, Y.; Michalow, K.; Matam, S.; Winkler, A.; Maeglia, A.; Yoona, S.; Heele, A.; Weidenkaffa, A.; Ferri, D. Methane abatement under stoichiometric conditions on perovskite-supported palladium catalysts prepared by flame spray synthesis. *Appl. Catal. B Environ.* **2014**, *144*, 631–643. [CrossRef]
68. Lu, Y.; Eyssler, A.; Otala, E.; Matam, S.; Brunko, O.; Weidenkaff, A.; Ferri, D. Influence of the synthesis method on the structure of Pd-substituted perovskite catalysts for methane oxidation. *Catal. Today* **2013**, *208*, 42–47. [CrossRef]
69. Auvray, X.; Lindholm, A.; Milh, M.; Olsson, L. The addition of alkali and alkaline earth metals to Pd/Al2O3 to promote methane combustion. Effect of Pd and Ca loading. *Catal. Today* **2018**, *299*, 212–218. [CrossRef]
70. Colussi, S.; Trovarelli, A.; Cristiani, C.; Lietti, L.; Groppi, G. The influence of ceria and other rare earth promoters on palladium-based methane combustion catalysts. *Catal. Today* **2012**, *180*, 124–130. [CrossRef]
71. Kang, T.; Kim, J.; Kang, S.; Seo, G. Promotion of methane combustion activity of Pd catalyst by titania loading. *Catal. Today* **2000**, *59*, 87–93. [CrossRef]
72. Bounechada, D.; Groppi, G.; Forzatti, P.; Kallinen, K.; Kinnunen, T. Effect of periodic lean/rich switch on methane conversion over a Ce–Zr promoted Pd-Rh/Al2O3 catalyst in the exhausts of natural gas vehicles. *Appl. Catal. B Environ.* **2012**, *119–120*, 91–99. [CrossRef]
73. Ersson, A.; Kušar, H.; Carroni, R.; Griffin, T.; Järås, S. Catalytic combustion of methane over bimetallic catalysts a comparison between a novel annular reactor and a high-pressure reactor. *Catal. Today* **2003**, *83*, 265–277. [CrossRef]
74. Kul Ryu, C.; Wong Ryoo, M.; Soo Ryu, I.; Kang, S. Catalytic combustion of methane over supported bimetallic Pd catalysts: Effects of Ru or Rh addition. *Catal. Today* **1999**, *47*, 141–147. [CrossRef]
75. Lyubovsky, M.; Smith, L.; Castaldi, M.; Karim, H.; Nentwick, B.; Etemad, S.; LaPierre, R.; Pfefferle, W. Catalytic combustion over platinum group catalysts: Fuel-lean versus fuel-rich operation. *Catal. Today* **2003**, *83*, 71–84. [CrossRef]
76. Oh, S.; Mitchell, P. Effects of rhodium addition on methane oxidation behavior of alumina-supported noble metal catalysts. *Appl. Catal. B Environ.* **1994**, *5*, 165–179. [CrossRef]
77. Yang, N.; Liu, J.; Sun, Y.; Zhu, Y. Au@PdOx with a PdOx-rich shell and Au-rich core embedded in Co_3O_4 nanorods for catalytic combustion of methane. *Nanoscale* **2019**, *9*, 4108–4109. [CrossRef]

78. Venezia, A.; Murania, R.; Pantaleo, G.; Deganello, G. Pd and PdAu on mesoporous silica for methane oxidation: Effect of SO_2. *J. Catal.* **2007**, *251*, 94–102. [CrossRef]
79. Miao, S.; Deng, Y. Au-Pt/Co_3O_4 catalyst for methane combustion. *Appl. Catal. B Environ.* **2001**, *31*, l1–l4. [CrossRef]
80. Lapisardi, G.; Urfels, L.; Gelin, P.; Primet, M.; Kaddouri, A.; Garbowski, E.; Toppi, S.; Tena, E. Superior catalytic behaviour of Pt-doped Pd catalysts in the complete oxidation of methane at low temperature. *Catal. Today* **2006**, *117*, 564–568. [CrossRef]
81. Larpisardi, G.; Gélin, P.; Kaddouri, A.; Garbowski, E.; Da Costa, S. Pt-Pd bimetallic catalysts for methane emissions abatement. *Top. Catal.* **2007**, *42–43*, 461–464.
82. Kinnunen, N.; Hirvi, J.; Suvanto, M.; Pakkanen, T. Methane combustion activity of Pd–PdOx–Pt/Al_2O_3 catalyst: The role of platinum promoter. *J. Mol. Catal. A Chem.* **2012**, *356*, 20–28. [CrossRef]
83. Bugosh, G.; Easterling, V.; Rusakova, I.; Harold, M. Anomalous steady-state and spatio-temporal features of methane oxidation on Pt/Pd/Al_2O_3 monolith spanning lean and rich condition. *Appl. Catal. B Environ.* **2015**, *165*, 68–78. [CrossRef]
84. Watanabe, T.; Kawashima, K.; Tagawa, Y.; Tashiro, K.; Anoda, H.; Ichioka, K.; Sumiya, S.; Zhang, G. *New DOC for Light Duty Diesel DPF System*; SAE Technical Paper Series; SAE: Warrendale, PA, USA, 2007.
85. Nomura, K.; Noro, K.; Nakamura, Y.; Yazawa, Y.; Yoshida, H.; Satsuma, A.; Hattori, T. Pd–Pt bimetallic catalyst supported on SAPO-5 for catalytic combustion of diluted methane in the presence of water vapor. *Catal. Lett.* **1998**, *53*, 167–169. [CrossRef]
86. Persson, K.; Jansson, K.; Järås, S. Characterisation and microstructure of Pd and bimetallic Pd–Pt catalysts during methane oxidation. *J. Catal.* **2007**, *245*, 401–414. [CrossRef]
87. Nassiri, H.; Hayes, R.E.; Semagina, N. Stability of Pd-Pt catalysts in low-temperature wet methane combustion: Metal ratio and particle reconstruction. *Chem. Eng. Sci.* **2018**, *186*, 44–51. [CrossRef]
88. Goodman, E.; Dai, S.; Yang, A.; Wrasman, C.; Gallo, A.; Bare, S.; Hoffman, A.; Jaramillo, T.; Graham, G.; Pan, X.; et al. Uniform Pt/Pd Bimetallic Nanocrystals Demonstrate Platinum Effect on Palladium Methane Combustion Activity and Stability. *ACS Catal.* **2017**, *7*, 4372–4380. [CrossRef]
89. Persson, K.; Ersson, A.; Jansson, K.; Fierro, J.; Jaras, S. Influence of molar ratio on Pd–Pt catalysts for methane combustion. *J. Catal.* **2006**, *243*, 14–24. [CrossRef]
90. Yamamoto, H.; Uchida, H. Oxidation of methane over Pt and Pd supported on alumina in lean-burn natural-gas engine exhaust. *Catal. Today* **1998**, *45*, 147–151. [CrossRef]
91. Semagina, N.; Nassiri, H.; Lee, K.; Hu, Y.; Hayes, R.E.; Scott, R.W.J. Water shifts PdO-catalyzed lean methane combustion to Pt-catalyzed rich combustion in Pd-Pt catalysts: In-situ X-ray absorption spectroscopy. *J. Catal.* **2017**, *352*, 649–656.
92. Nassiri, H.; Lee, K.; Hu, Y.; Hayes, R.E.; Scott, R.W.J.; Semagina, N. Platinum inhibits low-temperature dry lean methane combustion via palladium reduction in Pd-Pt/Al_2O_3: An in-situ X-ray absorption study. *ChemPhysChem* **2017**, *18*, 238–244. [CrossRef]
93. Chen, M.; Schmidt, L.D. Morphology and composition of Pt-Pd alloy crystallites on SiO_2 in reactive atmospheres. *J. Catal.* **1979**, *56*, 198–218. [CrossRef]
94. Willis, J.; Gallo, A.; Sokaras, D.; Aljama, H.; Nowak, S.; Goodman, E.; Wu, L.; Tassone, C.; Jaramillo, T.; Abild-pedersen, F.; et al. Systematic Structure–Property Relationship Studies in Palladium-Catalyzed Methane Complete Combustion. *ACS Catal.* **2017**, *7*, 7810–7821. [CrossRef]
95. Burch, R. Low NOx options in catalytic combustion and emission control. *Catal. Today* **1997**, *35*, 27–36. [CrossRef]
96. Persson, K.; Pfefferle, L.; Schwartz, W.; Ersson, A.; Järås, S. Stability of palladium-based catalysts during catalytic combustion of methane: The influence of water. *Appl. Catal. B Environ.* **2007**, *74*, 242–250. [CrossRef]
97. van Giezen, J.; Van den Berg, F.; Kleinen, J.; Van Dillen, A.; Geus, J. The effect of water on the activity of supported palladium catalysts in the catalytic combustion of methane. *Catal. Today* **1999**, *47*, 287–293. [CrossRef]
98. Toso, A.; Colussi, S.; Padigapaty, S.; de Leitenburg, C.; Trovarelli, A. High stability and activity of solution combustion synthesized Pd-based catalysts for methane combustion in presence of water. *Appl. Catal. B Environ.* **2018**, *230*, 237–245. [CrossRef]
99. Gélin, P.; Urfels, L.; Primet, M.; Tena, E. Complete oxidation of methane at low temperature over Pt and Pd catalysts for the abatement of lean-burn natural gas fuelled vehicles emissions: Influence of water and sulphur containing compounds. *Catal. Today* **2003**, *83*, 45–57. [CrossRef]
100. Ciuparu, D.; Katsikis, N.; Pfefferle, L. Temperature and time dependence of the water inhibition effect on supported palladium catalyst for methane combustion. *Appl. Catal. A Gen.* **2001**, *216*, 209–215. [CrossRef]
101. Ciuparu, D.; Pfefferle, L. Support and water effects on palladium based methane combustion catalysts. *Appl. Catal. A Gen.* **2001**, *209*, 415–428. [CrossRef]
102. Escandón, L.; Niño, D.; Díaz, E.; Ordóñez, S.; Díez, F. Effect of hydrothermal ageing on the performance of Ce-promoted PdO/ZrO2 for methane combustion. *Catal. Commun.* **2008**, *9*, 2291–2296. [CrossRef]
103. Gholami, R.; Alyani, M.; Smith, K. Deactivation of Pd Catalysts by water during low temperature methane oxidation relevant to natural gas vehicle converters. *Catalysts* **2015**, *5*, 561–594. [CrossRef]
104. Burch, R.; Urbano, F.; Loader, P. Methane combustion over palladium catalysts: The effect of carbon dioxide and water on activity. *Appl. Catal. A Gen.* **1995**, *123*, 173–184. [CrossRef]
105. Monai, M.; Montini, T.; Chen, C.; Fonda, E.; Gorte, R.; Fornasiero, P. Methane catalytic combustion over hierarchical Pd@CeO_2/Si-Al_2O_3: Effect of the Presence of Water. *ChemCatChem* **2015**, *7*, 2038–2046. [CrossRef]

106. Ciuparu, D.; Pfefferle, L.; Bozon-Verduraz, F. Oxygen Exchange between Palladium and Oxide Supports in Combustion Catalysts. *J. Phys. Chem. B* **2002**, *106*, 3434–3442. [CrossRef]
107. Burch, R.; Crittle, D.; Hayes, M. C-H bond activation in hydrocarbon oxidation on heterogeneous catalysts. *Catal. Today* **1999**, *47*, 229–234. [CrossRef]
108. Barrett, W.; Nasr, S.; Shen, J.; Hu, Y.; Hayes, R.; Scott, R.; Semagina, N. Strong metal-support interactions in Pd/Co3O4catalyst in wet methane combustion: In situ X-ray absorption study. *Catal. Sci. Technol.* **2020**, *10*, 4229–4236. [CrossRef]
109. Wanke, S.; Flynn, P. The sintering of supported metal catalysts. *Catal. Rev. Sci. Eng.* **1975**, *12*, 93–135. [CrossRef]
110. Abbasi, R.; Wu, L.; Wanke, S.E.; Hayes, R.E. Kinetics of Methane Combustion over Pt and Pt-Pd catalysts. *Chem. Eng. Res. Des.* **2012**, *90*, 1930–1942. [CrossRef]
111. Abbasi, R.; Huang, G.; Istratescu, G.M.; Wu, L.; Hayes, R.E. Methane oxidation over Pt, Pt:Pd and Pd based catalysts: Effects of pre-treatment. *Can. J. Chem. Eng.* **2015**, *93*, 1474–1482. [CrossRef]
112. Hayes, R.E.; Kolaczkowski, S.T. Mass and heat transfer effects in catalytic monolith reactors. *Chem. Eng. Sci.* **1994**, *49*, 3587–3599. [CrossRef]